Double-headed binding of myosin II to F-actin shows the effect of strain on head structure.

Alimohammad Hojjatian[§], Dianne W. Taylor[§], Nadia Daneshparvar[§], Patricia M. Fagnant[#], Kathleen M. Trybus[#] and Kenneth A. Taylor[§]

§Inst. of Molecular Biophysics, Florida State University, Tallahassee, Florida 32306
#Dept of Molecular Physiology & Biophysics, Univ. of Vermont College of Medicine, Burlington, VT 05405

Supplemental Movie Legends

Movie 1

Supplemental Movie 1 Legend. At the beginning the reconstruction showed in surface view with the region where the classification occurred placed axially in the middle facing the viewer. The reconstruction then rocks from left to right four times before stopping to zoom in at which point the atomic model appears and the reconstruction envelope becomes transparent. The view then rocks from left to right four more times before the envelope disappears leaving only the atomic model. The atomic model is colored as follows: Leading Head heavy chain (green); Trailing Head heavy chain (red); ELC (yellow); RLC (blue).

Table 1

Single particle CryoEM Study statistics: Data collection and Image processing

Data collection	**HMM**
Camera	DE-64
Magnification	29,000
Physical pixel size	1.28 Å
Calibrated pixel size	1.27 Å
Defocus range (μm)	-0.5 to -2.5
Voltage (kV)	300
Number of Frames	23
Dose per frame (e^-/A^2)	1.23
Motion correction	
Patch size (x,y)	(7,5)
Number of iterations	30
Tolerance	0.1
Frame of reference	15
Truncation	4

In-frame motion correction	yes
CTF estimation	
Software	CTFFIND4
Spherical aberration (mm)	2.7
Amplitude contrast	0.07
Max resolution (Å)	3
Min resolution (Å)	50
Defocus step (Å)	5
Tolerated Astigmatism (Å)	500
Phase shift (min,max,step)	(0,180,2.5)
Patch size	256
b-factor	NA
Minimum defocus (Å)	50
Maximum defocus (Å)	50,000
Reconstruction	**HMM**
Box size (pixels)	256
Number of Micrographs	1,413
Initial number of particles	~830,000
particles after 2D classification (cisTEM)	400,058
particles after 2D classification (Relion)	53,986
Final number of particles	53,986
Map overall resolution (Å)	17
FSC threshold	0.143
Reconstruction	**Actin-HMM (decorated actin)**
Box size (pixels)	420
Number of Micrographs	1,413
Number of Tubes	5,778
Inter-box distance (Å)	28
Initial number of segments	304,437
segments after 3D classification (unmasked)	50,203
segments after 3D classification (masked)	17,394/21,048/2,697/9,070
Final number of particles	17,394/21,048
Helical Refinement parameters	
Tube outer diameter (Å)	400
# of unique asymmetrical units	1
Initial twist (deg), rise (Å)	-167.4, 28.5
Central Z length (%)	30
Local twist search (min, max) (deg)	-175, -160
Local rise search (min, max) (Å)	25, 30
Averaged helical twist, rise (deg, Å)	-167.11, 28.49
Map overall resolution (Å) (mixed)	19
Map overall resolution (Å) (HMM)	19
Map overall resolution (Å) (shifted HMM)	13

FSC threshold	0.143
Model refinement parameters	
Map resolution (Å)	20
Start temperature (K)	298
Final temperature (K)	298
G-force scale factor	0.05
Minimization steps	5,000
Simulation steps	50,000
Phenix RSR cycles	5
Implicit solvent	No
Model Validation	
MolProbity score	3.14
Clashscore	100.01
Ramachandran Plot	
Favored (%)	84.37
Allowed (%)	15.43
Disallowed (%)	0.21

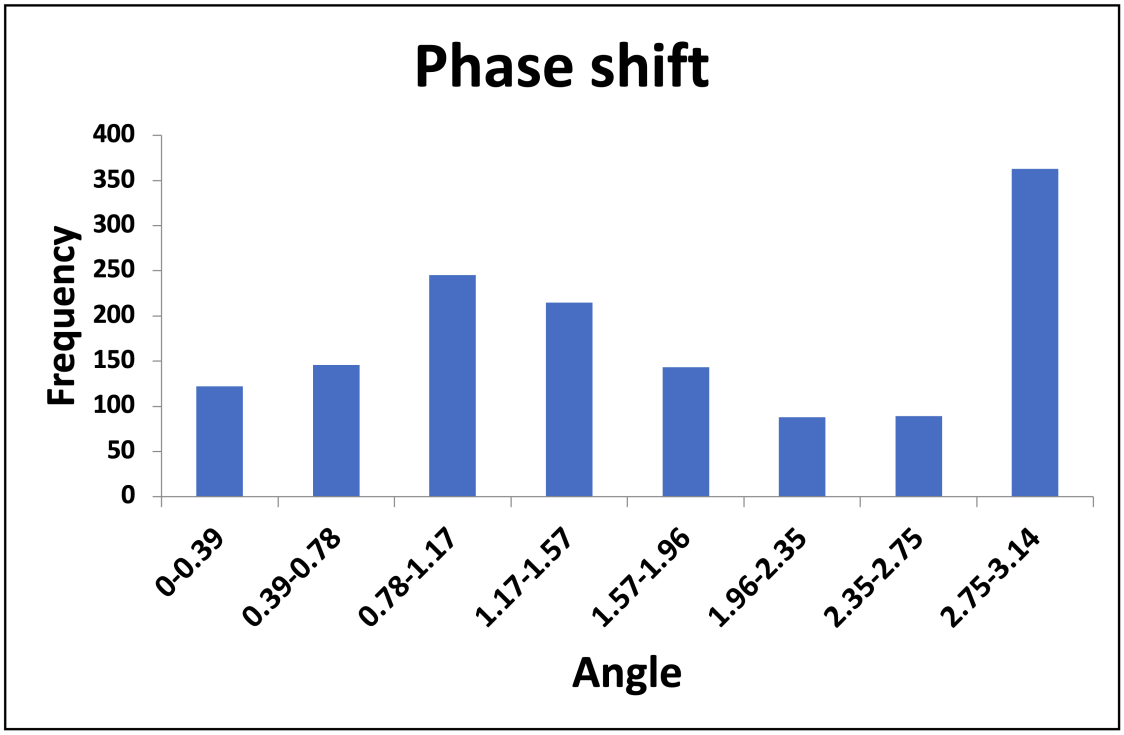

Supplemental Figure 1. Showing a histogram of the phase shifts determined by CTFFIND4 implemented in cisTEM.

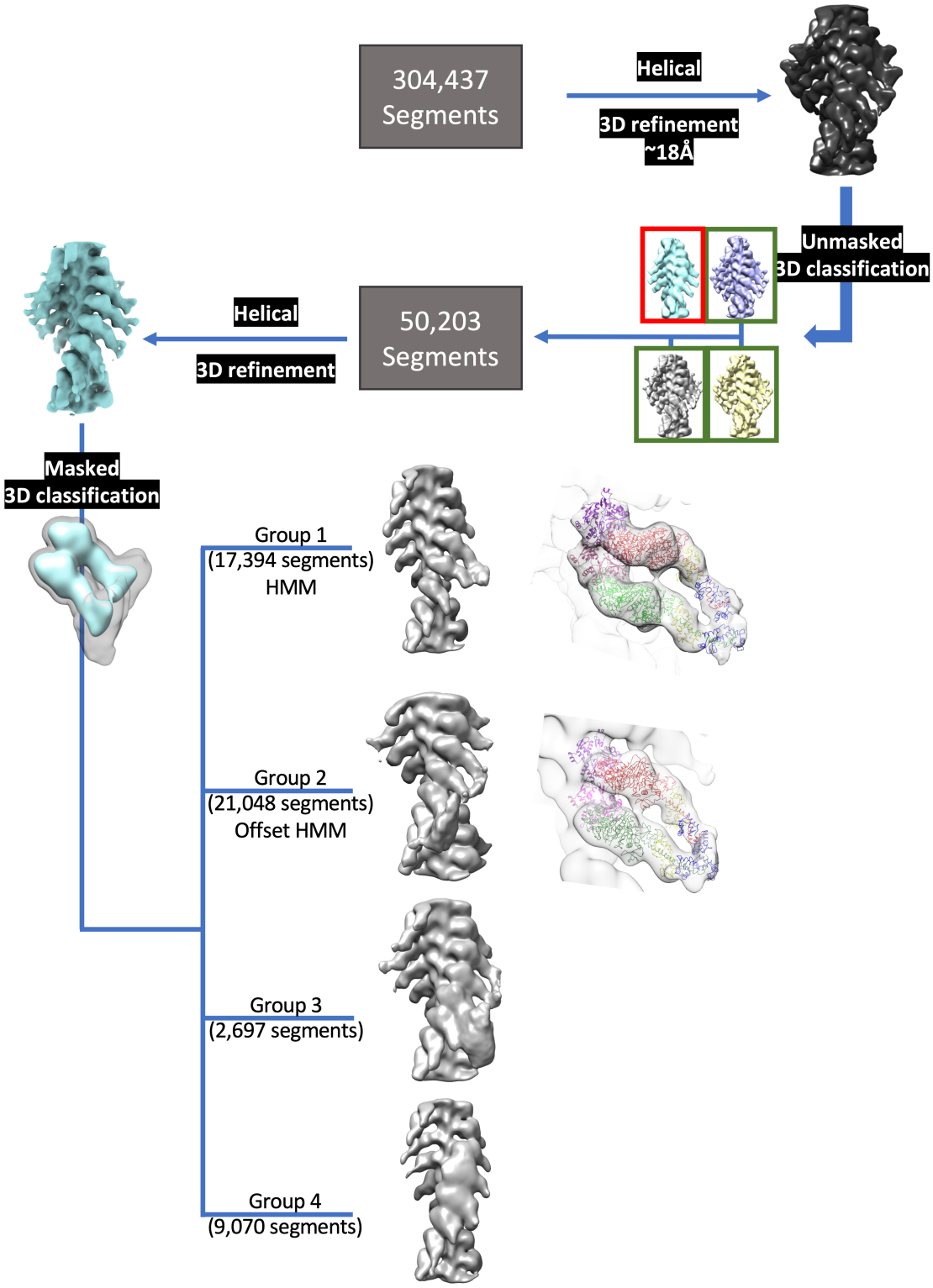

Supplemental Figure 2. Flow chart of the Single particle Acto-HMM image processing and fitting of the atomic model.

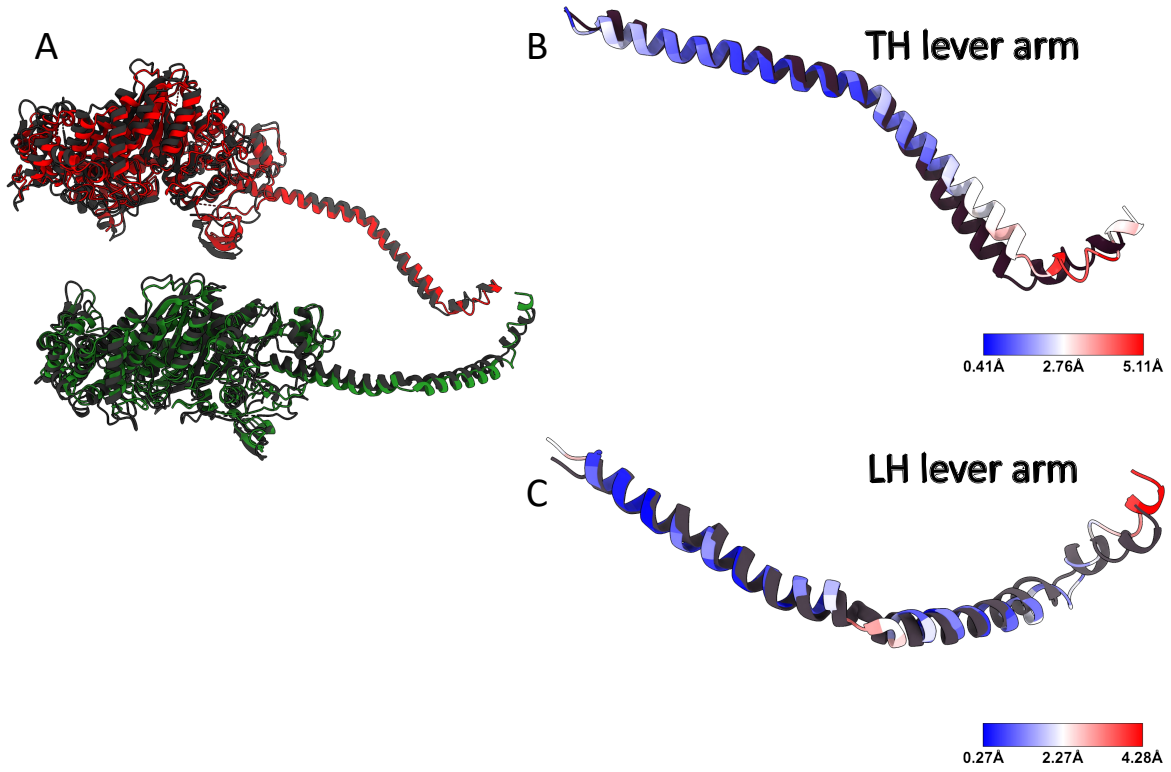

Supplemental Figure 3. RMSD heat map. (A) Showing a comparison between the models (heavy chains) before and after MDFF. The model before the flexible fitting is shown in dark grey, while the TH and the LH from the final model are shown in red and green, respectively. (B, C) Illustrating the conformational changes caused by MDFF in the lever arm of the TH and the LH, respectively. The magnitude of the conformational changes are shown using a heat map. Both heat maps, similarly, show an increase in separations at higher radii reaching a maximal separation close to the head-tail junction. In contrast to the Trailing head, the Leading head shows a high separation close to the junction between the ELC and RLC.

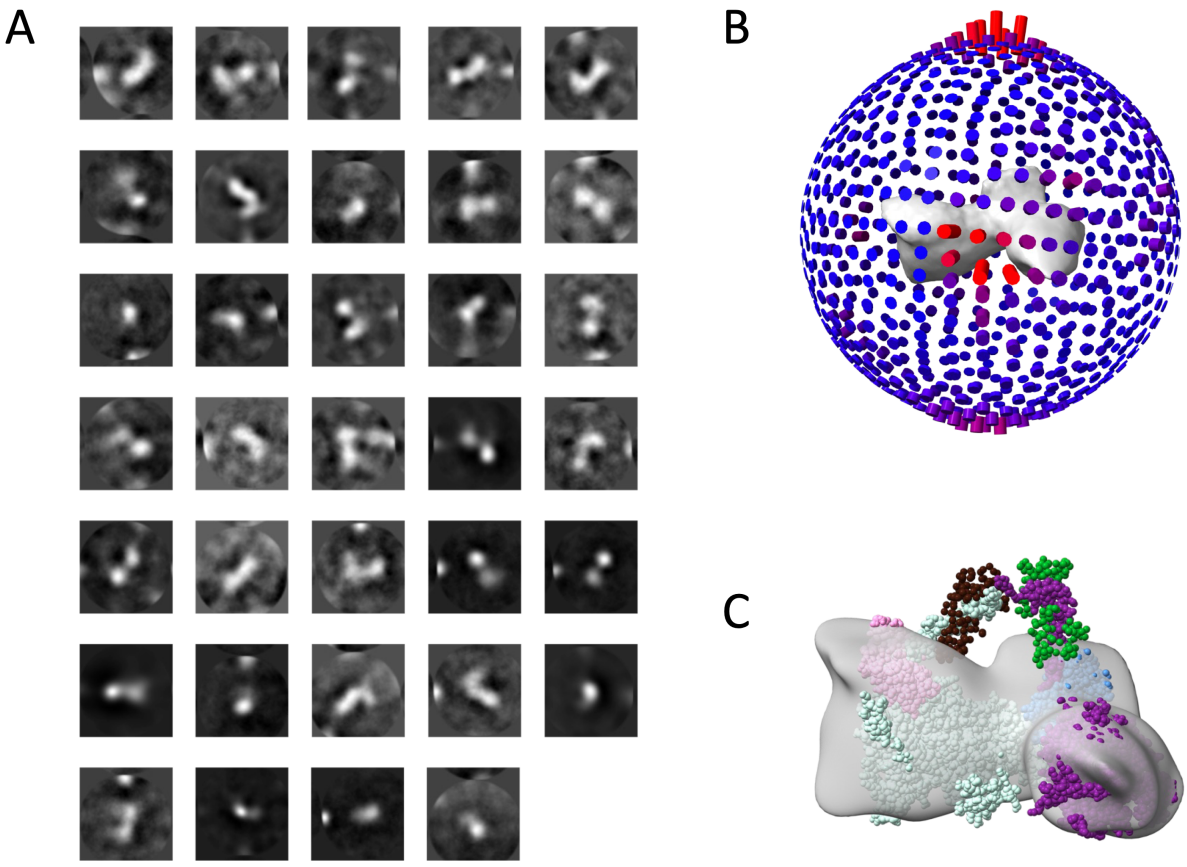

Supplemental Figure 4. Actin-free HMM molecules. (A) Class averages of individual HMM molecules. (B) distribution of orientations from the final 50,203 particles. Some orientation preference is visible. (C) Final reconstruction with the fitted atomic model showing a good fit of the motor domains and a lack of density for the light chains.

Discussion of Class averages obtained from Relion masked 3-D classification:

To recover the head-tail junction of the HMM molecules, we performed a masked 3-D classification limited to a pair of adjacent S1 heads (Fig. 2D), and without modification of the segment alignments. Twenty classes were produced and combined into four major groups based on similarity of features. Three out of the four groups from the 3-D classification show double-headed binding of HMM to F-actin (Suppl. Fig. 5). Group 1 (17,394 segments, 32% of 50,203 segments) included those classes with clear adjacency of the RLC regions and juxtaposition of the head-tail junction within the boundaries of the mask (Suppl. Fig. 5A-C). In this group, both heads, included in the mask appear to belong to the same HMM molecule. The Group 2 classes (21,048 segments, 39% of 50,203 segments) despite the clear presence of the two heads within the mask, do not show a clear proximity of their head-tail junctions. Instead, the two heads within the mask appear to come from different HMM molecules; the HMM head in the Leading position at the bottom of the mask appears to be paired to another head from outside of the mask just below it, and the Trailing Head at the top of the mask appears to be paired with another head just above it. In fact, the Trailing head pairing with the head just above it strongly resembles Class 1 (Suppl. Fig. 5A-C). Successive segments on each filament are offset by one actin subunit along the F-actin genetic helix while the HMM motif encompasses a pair of actin subunits along the long pitch helix (Suppl. Fig. 5D-F). Thus, for each HMM motif, there is a near duplicate HMM shifted axially ± one actin subunit along the long pitch helix. Group 3 classes (2,697 segments, 5% of 50,203 segments) is somewhat similar to Group 2, but can be distinguished by the presence of the stronger density for the head in the Trailing position (upper) and noisier density for the head in the Leading position (lower) within the mask (Suppl. Fig. 5G-I). This lower head extends well beyond the mask (Suppl. Fig. 5H, I). The map density for the upper head plus the one just above it appears very similar to the upper head in Group 2. Group 4 classes (9,070 segments, 17% of 50,203 segments) represents the segments with truncated lever-arm densities. We consider these segments as possibly representing single-headed binding by HMM (Suppl. Fig. 5J-L). No classes were observed completely lacking myosin head decoration for either of the two adjacent actin subunits. The S2 domain was not resolved in any of the 3-D class averages and is at best blurry even in 2D class averages (Fig. 2B). The inability to resolve the S2 domain could be due to both disorder relative to the RLCs and insufficient resolution.

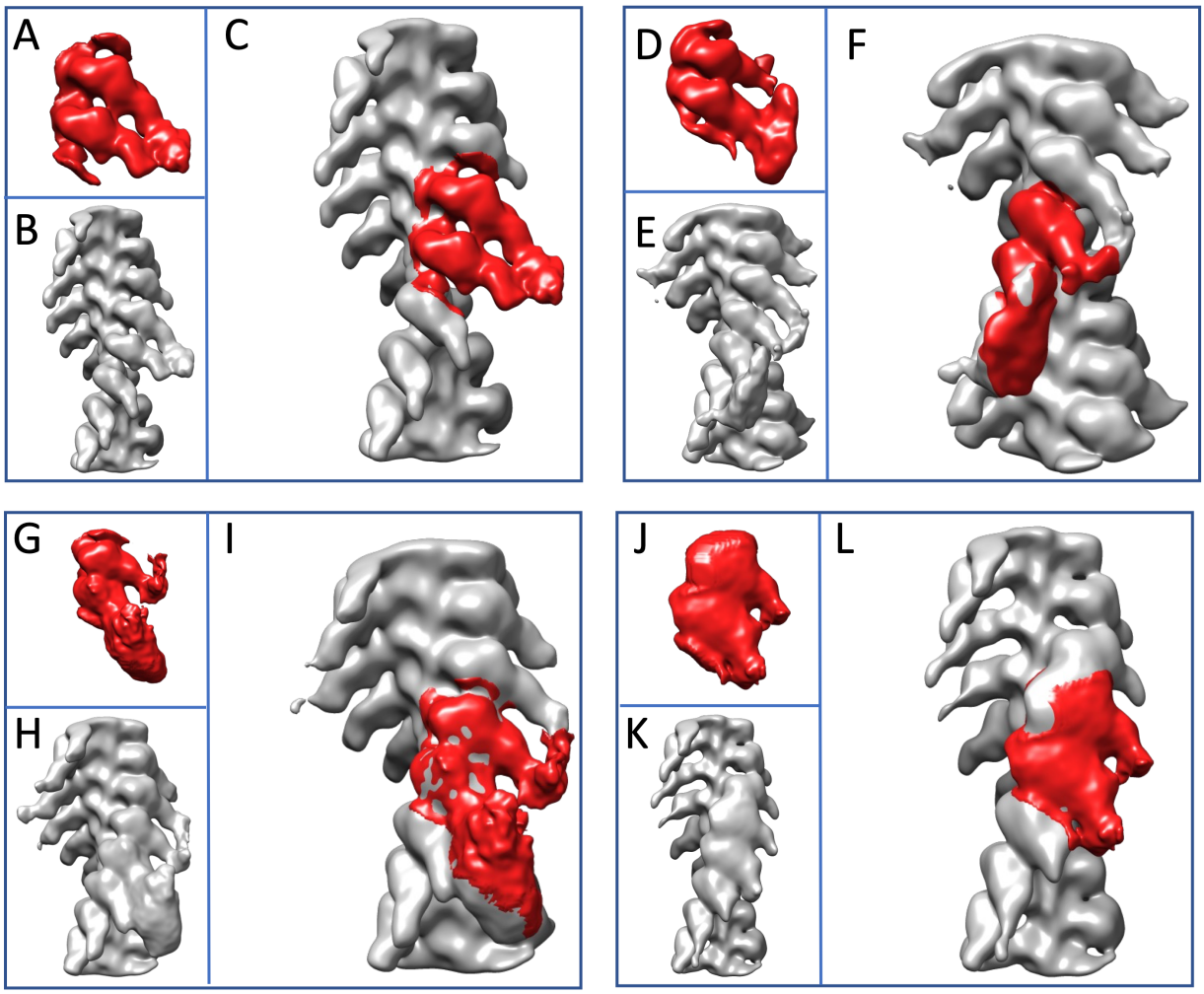

Supplemental Figure 5. The four major HMM class averages using the mask, shown in Figure 3D. (A-C) Group 1 class average. (A) Segmented acto-HMM density. (B) Entire 3D reconstruction volume of the Group 1 segments. (C) Superposition of (A) and (B). (D-F) Group 2 class average. (D) Segmented Group 2 acto-HMM density. (E) Entire 3D reconstruction volume of the Group 2 segments. (F) Superposition of (D) and (E). (G-I) Group 3 class average. (G) Segmented Group 3 acto-HMM density. (H) Entire 3D reconstruction volume of the Group 3 segments. (I) Superposition of (G) and (H). (J-L) Group 4 class average. (J) Segmented Group 4 acto-HMM density. (K) Entire 3D reconstruction volume of the Group 4 segments. (L) Superposition of (J) and (K).

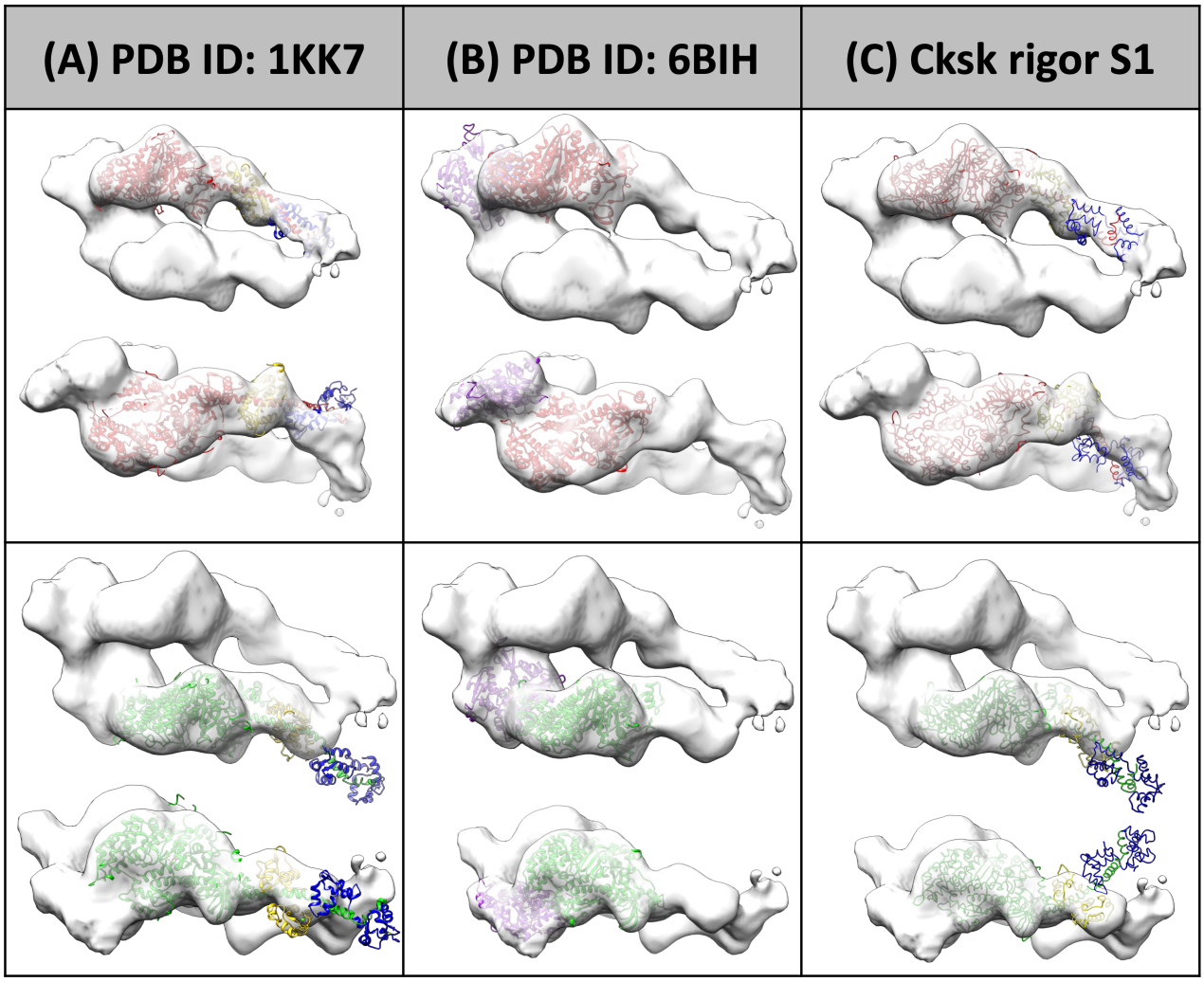

Supplemental Figure 6. Rigid body fitting of the motor domains from various myosin models in the nucleotide free state into the density map. The Trailing Head heavy chain is colored red, the Leading Head heavy chain is colored green. The ELC is yellow and the RLC blue. The upper panel shows an axial view (top) and a transverse view (bottom) of the Trailing Head. The lower panel shows equivalent views for the Leading Head. (A) Crystal structure of scallop myosin S1 in the near rigor conformation. (B) Cryo-EM structure of chicken smooth muscle myosin motor domain in the rigor state. (C) Cryo-EM structure of chicken skeletal S1 in the rigor state.

Codes and scripts

Production of simulated density map using atomic model (PDB ID: 1i84):
e2pdb2mrc.py --apix=1.28 --res=30 --box=256 --center 1i84-cut.pdb 1i84-cut-centered.mrc

production of the 2D projections of the simulated map:
relion_project --i 1i84-cut-centered.mrc --o projections --nr_uniform 30

script used for template-based particle picking using the 2D projections for the HMM that did not bind actin:
Gautomatch-v0.53_sm_20_cu8.0_x86_64 --apixM 1.28 --diameter 250 -T projections.mr
cs --apixT 1.28 micrographs/*ex-a.mrc --lp 30 --lsigma_cutoff 1.21 --hp 800 --lsigma_D 600 --lave_max 1 --lave_min -2 --min_dist 200 --cc_cutoff 0.38